International Journal of Microwave and Wireless Technologies, 2013, 5(1), 55–64.
doi:10.1017/S1759078712000815

RESEARCH PAPER

Antenna-in-package (AiP) in mm-wave band

MAHMOUD ALHENAWY AND MARTIN SCHNEIDER

We studied the viability of the embedded wafer level ball grid array (eWLB) package environment as an antenna platform for 77 GHz automotive radar sensors and the effects of package fabrication tolerances on the antenna performance. The investigation of different antenna concepts in the eWLB package and their characterization methods are addressed. The design procedures for electrically large, differentially fed loop antennas in a multilayer package structure are introduced. Two different planar antennas are developed and measured in an eWLB package showing promising results such as a gain of 9 GHz and an impedance bandwidth of 8 GHz. An acceptable antenna performance is recorded within the tolerance limits. Therefore, the eWLB package is seen as an appropriate platform for mm-wave antennas and as a good candidate for an antenna-in-package (AiP) concept.

Keywords: Antenna design, Modelling and measurements, Radar application

Received 1 June 2012; Revised 20 November 2012

I. INTRODUCTION

The millimeter wave (mm-wave) band widens the horizon for diverse radio frequency (RF)-frontend integration concepts such as antenna-on-chip (AoC), antenna-in-package (AiP), and system-in-package (SiP) to utilize the inherent small size of the antenna. Furthermore, technologies for circuit design and modeling can currently provide SiGe heterojunction bipolar transistors (HBTs) with operating frequencies up to 200 GHz. Therefore, highly integrated RF-frontends are developed to operate in the license-free band at 60 GHz for high data rate communication systems and for the 77 GHz band for automotive radar sensors [1, 2]. In [3], high data rate wireless communication systems that deliver up to 20 Gbit/s are investigated at 120 GHz. Such systems call for low profile, high gain, efficient antennas for portable devices.

Currently, automotive radar sensors, either for long range, medium range, or short range, are based on planar antennas on printed circuit board (PCB) and microwave monolithic integrated circuits (MMIC). Wire-bonds are used to interconnect the antenna system and its feeding MMIC, which are assembled in a cavity grooved in PCB. Although, the output of the MMIC is differential, single-ended antennas are used and hence a transition is introduced to match the two modes. The assembly of the radar frontend using these traditional discrete components demands an accurate and precise processing. Further development of such sensors has moved in the direction of simplifying its fabrication process while keeping the same level of reliability and precision. In addition, the minimization of the insertion loss, e.g., elimination of bonding wires, can be achieved by increasing the system integrability. Therefore, new antenna concepts and system integration techniques are sought. In AoC concepts, antennas are usually labeled with low radiation efficiencies due to the low resistivity substrates. In [2], a radar transceiver with an AoC concept is developed on a thin, low resistivity silicon substrate. The use of the antenna alone on the thin silicon substrate leads to an efficiency of 10%. Therefore, a second parasitic patch is stacked, mounted on quartz glass, on the first patch that leads to a total antenna efficiency of about 50% at 77 GHz. There are different approaches to enhance the efficiency of such antennas, such as backside micro-machining and/or the addition of an extra dielectric layer on top of the die [4, 5]. Parallel to the ongoing research to improve the performance of AoC concepts, AiP concepts are quite an active topic that can provide a good solution for efficient mm-wave antennas [6, 7].

Embedded wafer level ball grid array (eWLB) is a die packaging technique developed by Infineon [8–10]. In [6], we demonstrated that it can be used as an antenna platform. In this paper, we further study the package environment for the enhancement of the antenna performance and the integration of more than one radiating element per package. This work is structured as follows: In section I, the concept of antennas in eWLB package is briefed and a characterization mechanism for passive antennas in an eWLB package is presented. In section III, the effects of the package fabrication tolerance and the perturbation of the originally spherical soldering balls on the antenna performance are studied. In addition, a parametric study for the locations of the antenna within the package and its performance over frequency is carried out. In section IV, the design procedures for electrically large loop antennas in a multilayer package environment are discussed. In addition, the design of a printed dipole antenna (PDA) backed with a reflector and a director on top as well as the design of four PDAs in one

Institute of Telecommunications and High-Frequency Techniques, RF & Microwave Engineering Laboratory, University of Bremen, Bremen, Germany. Phone: +4942121862417
Corresponding author:
M. Alhenawy
Email: mahmoud.alhenawy@hf.uni-bremen.de

eWLB package are presented. Furthermore, measurements of printed loop antenna (PLA), PDA, and tilted-PDA, using the introduced measurement concept, are presented. Finally, measurement results for the AiP with a dielectric lens are discussed.

II. AIP CONCEPT

In this section, the eWLB package environment is summarized and the employed AiP concept is introduced. Furthermore, a measurement concept that is used for the antenna characterization is developed.

A) eWLB package architecture

Figure 1(a) shows a schematic diagram for the package architecture that mainly consists of two layers, namely the mold compound and a dielectric layer [9]. The mold compound has a relative permittivity of $\varepsilon_r \approx 3$ and a loss tangent of $\tan\delta \approx 0.005$ at 77 GHz. The dielectric layer has a relative permittivity of $\varepsilon_r \approx 3.6$ and a loss tangent of $\tan\delta \approx 0.026$ measured at 1 GHz. The mold compound has a thickness of 450 μm and the dielectric layer has an overall thickness of about 17 μm. The thickness of the dielectric layer varies based on the location of the chip and the redistribution layer (RDL) as well. In the eWLB packaging concept, the pads of the die in the fan-in area, limited to the size of the die, is mapped to an arbitrary pad pitch in the fan-out area. This redistribution or mapping is realized in the dielectric layer using a thin film copper layer called the RDL shown in Fig. 1(a). Indeed, eWLB packages were fabricated with different sizes such as 8×8 mm² and 8×12 mm² for our investigation. In addition, a single eWLB package can combine two dies or more that can be interconnected through the RDL. Figure 1(b) shows the MMIC and the antenna system integrated in one eWLB package and hence there is no need for 77 GHz connections outside the package. The antenna system is patterned into the thin film copper layer in the RDL, which can also be used to make a transmission line to interconnect the antenna and the MMIC as indicated in Fig. 1(b). In addition, on top of the PCB carrier and beneath the antenna, there is a copper plate that acts as a shield for the PCB and a reflector for the antenna system. The antenna radiates through the mold compound in the broadside direction.

B) Radiating elements

In eWLB packaging technology, the RDL can be a single or a double layer. Only a single layer RDL is considered in the ongoing design. Utilizing one metalization layer, differential antennas fed with a coplanar stripline (CPS) such as loop antennas, dipole antennas, folded dipoles, Vivaldi antennas, and coplanar patch antennas can be designed. Although, single-ended antennas fed with a coplanar waveguide transmission line (CPW) such as patch antennas and bowtie antennas are attainable, the current designs are limited to differential antennas as the used MMIC has a differential output. Antennas in eWLB package can be backed with a reflector on the PCB and/or directors patterned on top of the mold compound.

In the ongoing investigation of the viability of the eWLB package as an antenna platform, antennas are characterized independently from the chip. In other words, the silicon die is a dummy chip and it is not connected neither to the antenna nor to its DC biasing. It is included to examine its geometrical and electrical characteristics on the antenna performance. Figure 2 depicts the used model where the antenna is fed from an external source. The silicon chip is modeled as a die that has a relative permittivity of $\varepsilon_r = 11.9$, a resistivity of $\varrho = 18\,\Omega$ cm, and an overall dimension of $3.0 \times 3.0 \times 0.4$ mm³. In the next section, we focus on two types of antennas that radiate in the broadside direction, namely: the loop antenna and the dipole antenna. Such antennas will radiate in both directions perpendicular to their planes and therefore it is necessary to back each antenna with a reflector on the PCB.

C) Measurement concept

Figure 3 depicts the proposed measurement concept, where an AiP will be soldered on an evaluation board that is interfaced to the measurement equipment. Evaluation boards are designed as an interface between the eWLB package and the measurement device. Since the Si-chip is a dummy chip and the antenna is fed from an external source as depicted in Fig. 2, RF-transitions are developed to transfer the 77 GHz-signal to/from the package (RF-T1) and to/from the measurement equipment (RF-T2) as well. The RF signal is differentially carried in the eWLB package with a CPS transmission line and on the PCB with a conductor-backed coplanar stripline (CB-CPS) transmission line. Both transmission lines are designed with a characteristic impedance of $Z_o = 100\,\Omega$. Figure 4 shows the first transition RF-T1 that interfaces the eWLB package and the PCB. It converts the differential signal carried by a CPS in the package to a differential signal carried by a CB-CPS on the PCB. It utilizes the soldering balls to guide the RF signal. The CPS in the package is optimized to minimize the stray radiation in the end-fire direction while the CB-CPS on the PCB employs a

Fig. 1. SiP concept. (a) An embedded water level ball grid array (eWLB) package and (b) eWLB package and integrating an antenna and a chip.

https://doi.org/10.1017/S1759078712000815 Published online by Cambridge University Press

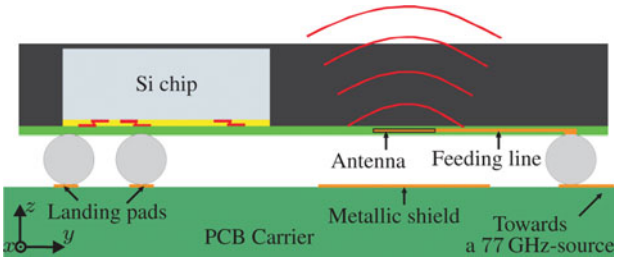

Fig. 2. Passive AiP.

quarter-wavelength transformer for impedance matching. Soldering balls, close to the transition zone, are removed to avoid undesired coupling.

A row of vias, marked in blue in Fig. 4, is used to ground the landing pads of the balls around the transition. In a complete design of an evaluation board, these vias are extended to ground the antenna reflector mounted on the PCB. Figure 4 shows the simulation results of the developed transition RF-T1 for the differential mode excitation. The transition is well matched over a wide frequency range including the range of interest from 76 to 81 GHz. Quite acceptable performance is observed in this range such as an insertion loss of 0.8 dB at 76.5 GHz. Moreover, 50% of the recorded insertion loss is due the radiation induced by the discontinuity over the transition. Since the transition is symmetric, there is no coupling between the differential mode and the common mode. This is expressed in the simulation result by an isolation better than 40 dB due to the numerical approximation.

The second RF-transition RF-T2 is to interface the evaluation board to the measurement equipment. There are several techniques to develop this transition such as the usage of a balun and a single-ended finline or direct usage of a differential finline [6]. In [11], our developed differential finline transition has a wideband impedance bandwidth of about 37 GHz and an insertion loss less than 0.5 dB, which allows a precise characterization of the device under test. Finally, a wafer prober station is used for the measurement of the reflection coefficients of the antennas while their radiation patterns are measured in an anechoic chamber.

III. PACKAGE ENVIRONMENT PARAMETRIC STUDY

This section includes the study of the fabrication tolerance on the antenna performance and the optimization of the antenna location within the package. Also, the characterization of the antenna performance over the frequency range of interest is included.

A) Mold compound and soldering balls

The thickness and the size of the mold compound plays a major role in forming the radiation pattern and the efficiency

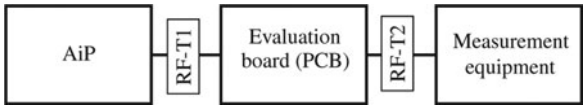

Fig. 3. Measurement concept.

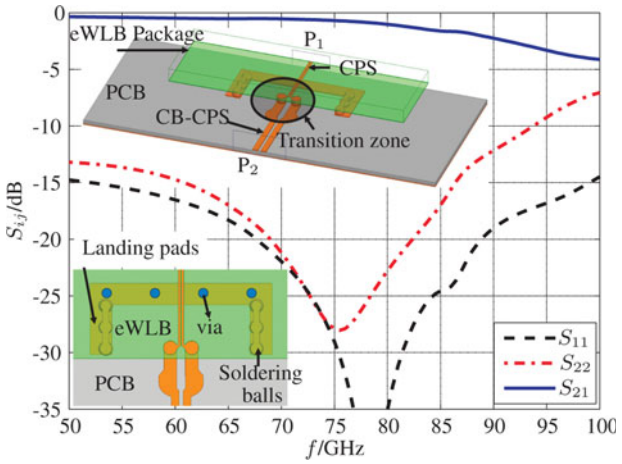

Fig. 4. RFT1 and its scattering parameters.

of the antenna. Therefore, the acceptable thickness of the mold is investigated for a fixed package size. Figure 5 shows how the gain of a PLA varies versus the thickness of the mold compound t_m in the broadside direction, i.e., $\theta = 0^\circ$, at 76.5 GHz. It also reveals a continuous decrease in the directivity in the broadside direction with almost a constant efficiency. Increasing the thickness of the mold creates a dip in the broadside direction which splits the main lobe into two beams. For example, at a mold thickness $t_m = 940\,\mu$m, the dip splits the main beam into two beams with maxima at $\theta = \pm 30^\circ$, not shown. The smaller the mold thickness, the better the performance of the antenna, but the minimum thickness is limited by the die height. The fabricated samples have a mold thickness of 450 μm with a tolerance of $\pm 20\,\mu$m, which leads to a maximum gain drift of 1 dB. Furthermore, the resonance frequency of the antenna is insensitive to the tolerance of mold compound, results are not shown here.

The soldering balls have a pitch of 500 μm and a conductivity of $\sigma = 7$ MS/m. Generally, soldering balls can be utilized for a wide variety of functions such as DC biasing, intermediate frequency (IF) transmission, RF transmission, heat transfer, and mechanical stability of the package. In the current design, two balls are employed in the transition RF-T1 and a grid of balls, distributed on the outer border of the package, are connected through the RDL and also on the PCB level to form a cavity beneath the antenna as shown in

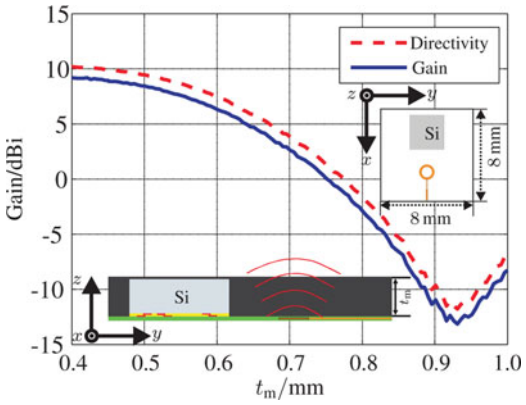

Fig. 5. Gain versus mold thickness at 76.5 GHz

https://doi.org/10.1017/S1759078712000815 Published online by Cambridge University Press

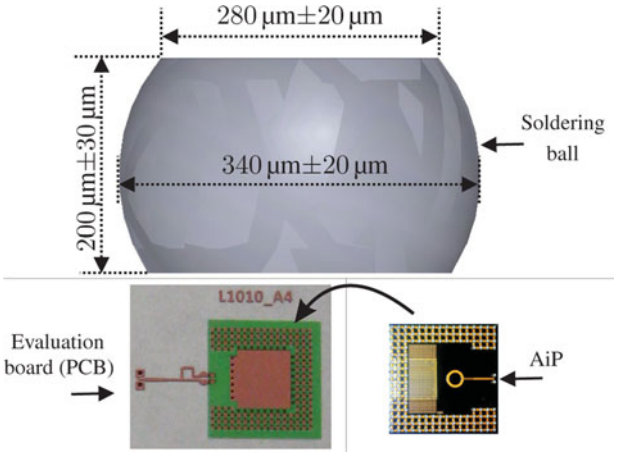

Fig. 6. Soldering ball and evaluation board.

Fig. 6. Our designed antennas are based on soldering balls with a height of $h_b = 200$ µm among other two possible options of 150 and 250 µm. The nominal height value is 200 µm with a soldering tolerance of about ±30 µm. After soldering, the spherical shape of the balls turns into an oval shape with different diameters as depicted in Fig. 6. The effect of the ball height variation on the antenna gain is plotted in Fig. 7 (a). It shows a robust performance with a maximum drift of about 0.5 dB. The soldering tolerance with respect to the diameters of the balls has a negligible effect on the antenna performance. However, changing the height of the balls has remarkable effects on the reflection coefficient of the antenna as shown in Fig. 7(b). It shows that the resonance frequency of the antenna is shifted back and forth by about 3 GHz in response to a tolerance of ±30 µm around the nominal value. Such deviation could limit the usability of the antenna; however, the measurement of the balls' height after soldering for different samples and charges shows an actual tolerance of ±5 µm, which causes an acceptable deviation of about 400 MHz around the desired resonance frequency.

B) Dielectric and RDL layers

The dielectric layer consists of two layers, namely Diel. I and Diel. II, as shown in Fig. 8(a). The fabrication tolerance of the dielectric layer thicknesses ranges from ±1.0 to ±3.0 µm. In the tolerance analysis, the performance of the PLA is observed versus variation. The PLA is designed at a resonance frequency of 78 GHz. The part of the Diel. II on top of the RDL layer has a fabrication tolerance of ±3 µm which results in a shift in the resonance frequency by about 200 MHz as shown in Fig. 8(a). Figure 8(b) shows that the thickness variation of Diel. I has a negligible effect on the resonance frequency. Figure 8(c) shows a dominant drift in the resonance frequency, in the order of 500 MHz, appears when the thickness of the Diel. II on Diel. I varies by ±1 µm. The thickness of the thin film RDL layer has a fabrication tolerance of ±1.5 µm. On the one hand, decreasing the RDL thickness has a slight effect on the antenna performance, but on the other hand, the increase of the thickness causes a drift in the resonance frequency by about 500 MHz to the left side as shown in Fig. 8(d). The radiation pattern of the PLA is insensitive to the variation of the dielectric and the RDL layer within the tolerance limits. Moreover, the simulation results show that the antenna efficiency is reduced by 8 percentage points due to the loss in this dielectric layer.

C) Radiation pattern versus frequency

The frequency range of interest for automotive radar sensors is from 76 to 81 GHz. Therefore, the radiation pattern and the effects of the lossy silicon chip on the antenna performance are investigated over this range. Figures 9 and 10 show simulation results for the PLA with and without the dummy Si-chip over the frequency range from 76 to 81 GHz. They show that as the frequency increases, the gain decreases, e.g., the difference between the gain at 76 GHz and at 81 GHz is about 1.5 dB. Figures 9(a) and 9(b) also show a slight change over frequency in the E-plane of the antenna pattern at the package edge, i.e., $\vartheta = 90°$. Since the Si-chip lies in the H-plane of the antenna, its effects are more pronounced in shaping the pattern in the H-plane compared to the E-plane. Although the Si-chip slightly reduces the antenna efficiency, it sharpens the main beam across its H-plane.

D) Si-chip Location in an eWLB Package

The location of the Si-chip in the package is crucial for the performance of an AiP. Therefore, a parametric study for the distance between the antenna and the dummy chip is carried out.

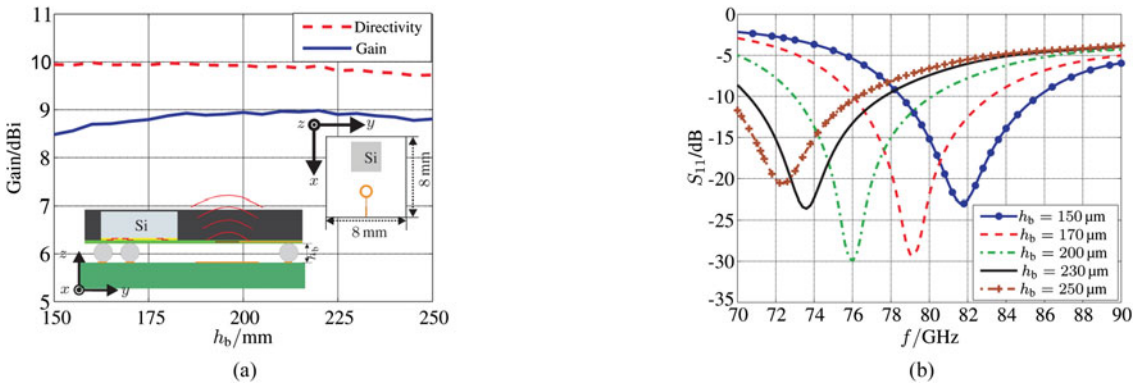

Fig. 7. Effects of the soldering balls' height variation on the antenna performance by 3D simulation. (a) Antenna gain versus soldering balls' height at 76.5 GHz and (b) antenna reflection coefficient versus balls' height.

https://doi.org/10.1017/S1759078712000815 Published online by Cambridge University Press

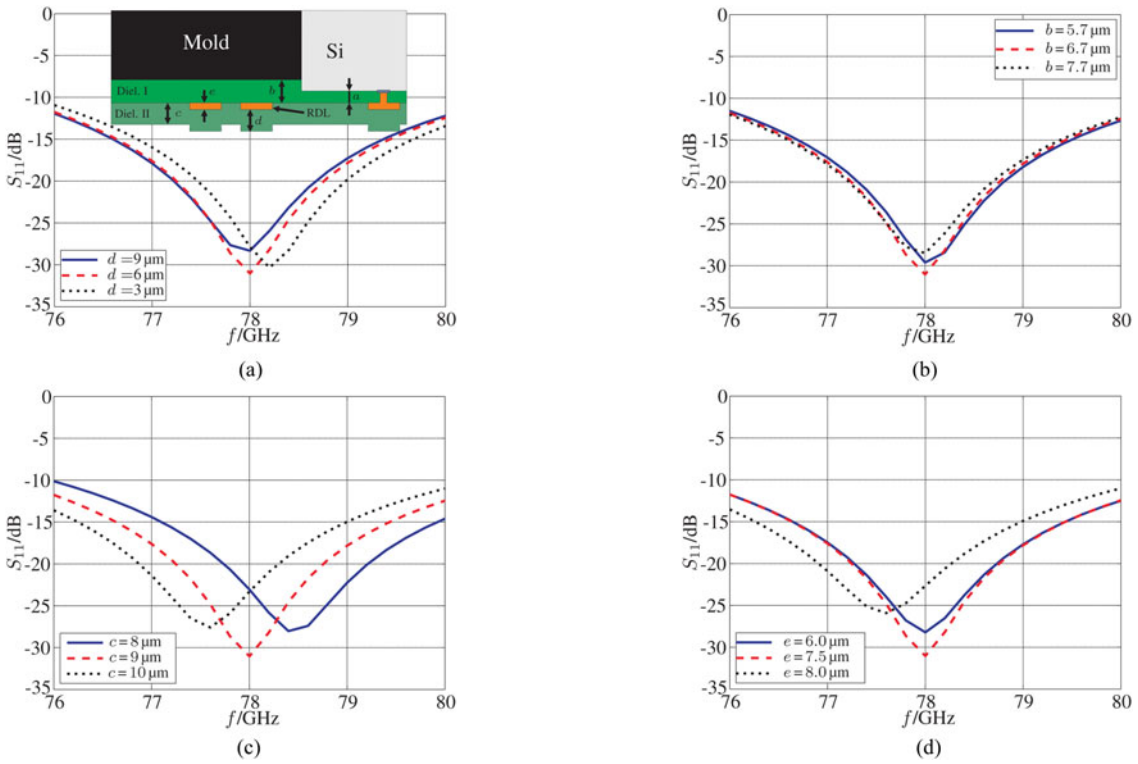

Fig. 8. Tolerance analysis for a PLA in an 8 × 8 mm² package using 3D simulation. (a) S_{11} versus the thickness of Diel. II on RDL, (b) S_{11} versus the thickness of Diel. I, (c) S_{11} versus the thickness of Diel. II on Diel. I, and (d) S_{11} versus the thickness RDL.

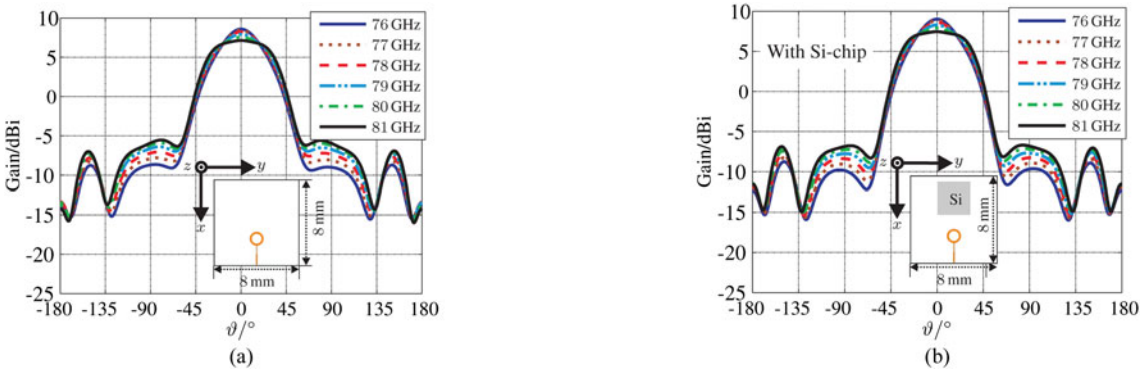

Fig. 9. E-plane pattern versus frequency and effects of dummy Si-chip in 8 × 8 mm² package size. (a, b) Radiation pattern along the E-plane (i.e., *yz*-plane).

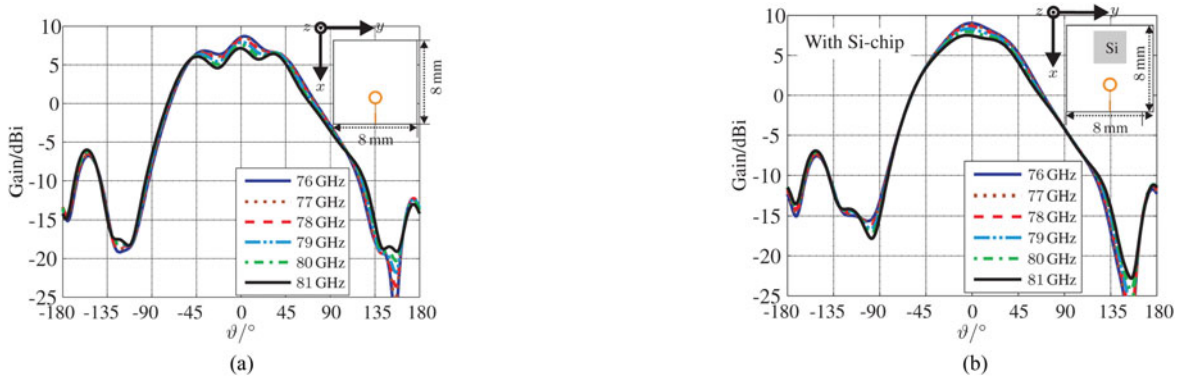

Fig. 10. H-plane pattern versus frequency and effects of dummy Si-chip in 8 × 8 mm² package size. (a, b) Radiation pattern along the H-plane (i.e., *xz*-plane).

https://doi.org/10.1017/S1759078712000815 Published online by Cambridge University Press

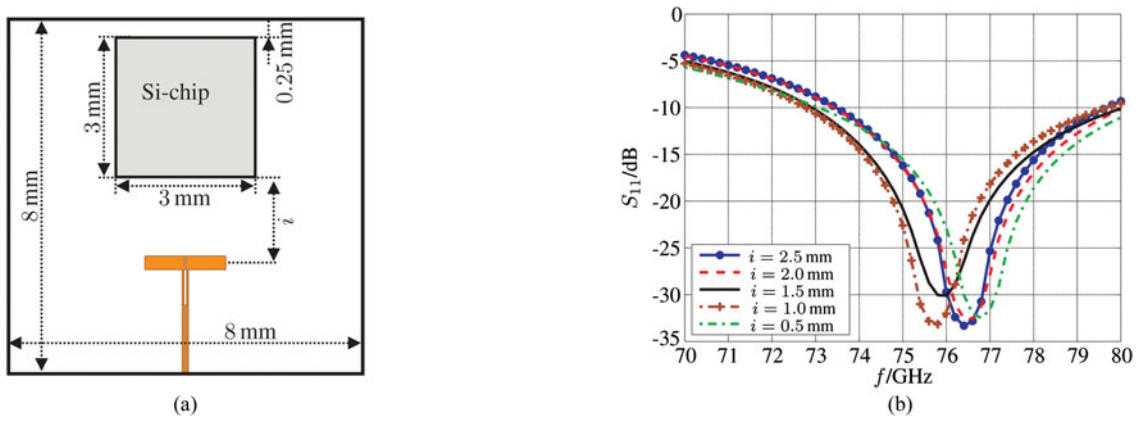

Fig. 11. I. Parametric study of the antenna location in an 8 × 8 mm² package using 3D simulation. (a) Simulated eWLB package and (b) Reflection coefficient.

Figure 11(a) shows the studied configuration. Figure 11(b) shows that changing the distance i between the antenna and the Si-chip leads to a shift in the resonance frequency of about 500 MHz. This shift in the resonance frequency can be compensated in a redesign. The effects of changing the distance between the antenna and the chip is more pronounced on the antenna radiation pattern and its efficiency η as shown in Figs. 12(a) and 12(b). The closer the antenna is to the chip, the lower the gain and the efficiency will be as well. The efficiency is decreased as more energy is coupled to the low resistivity silicon substrate. There are two factors that contribute to the gain reduction: firstly, the energy lost in the chip body, i.e., decreased efficiency. Secondly, the geometrical effect of the chip on the radiation pattern as the main beam becomes more flat in the boresight direction. For instance, when the distance between the chip and the antenna is $i = 2.5$ mm, the antenna has a gain and an efficiency of 9.3 dBi and 80% at 76.5 GHz, respectively. In comparison, at a distance $i =$ 0.5 mm, the gain and the efficiency are recorded to be 5.5 dBi and 45% at 76.5 GHz, respectively. If the chip were active, the antenna could be placed farther than 2.5 mm and up to 3.5 mm. However, in the current configuration, the distance i is determined to be 2.0 mm to minimize the undesired coupling between the antenna and both the Si-chip and the RF-transition RF-T1.

IV. ANTENNA DESIGN AND MEASUREMENT

In this section, the design procedures for an electrically large loop antenna are discussed. Furthermore, the design of four PDA within one package is introduced. In addition, the improvement of the antenna gain as well as its radiation pattern are discussed. Finally, measurement results using the developed measurement concept are presented.

A) Printed loop antenna (PLA)

A loop antenna has two different modes of radiation: it can radiate in either the end-fire or in the broadside direction. A loop antenna is classified as electrically small when its perimeter C is less than one-tenth of the operating wavelength λ. Such loops radiate in the end-fire direction while electrically large loops, where $C \geq \lambda$, radiate in the broadside direction. Although small loops are inefficient radiators, they could be used for inter-package communication. In electrically large loops, the electrical current is no longer uniformly distributed on the perimeter and therefore its main lobe departs the plane of the antenna toward the broadside direction. Indeed, the size of the loop that corresponds to a maximum gain in the broadside direction and its input impedance should be determined in order to design a matching network. Therefore, we

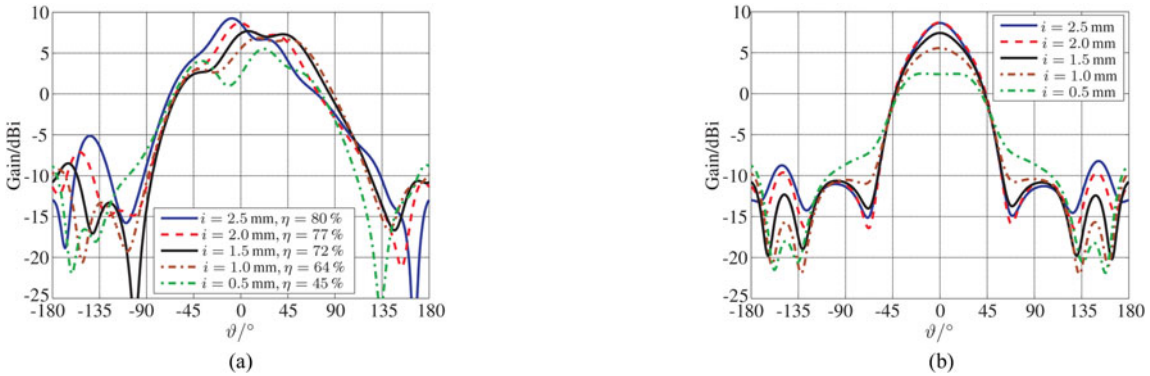

Fig. 12. II. Parametric study of the antenna location in an 8 × 8 mm² package using 3D simulation. (a) H-plane radiation pattern at 76.5 GHz and (b) E-plane radiation pattern at 76.5 GHz.

https://doi.org/10.1017/S1759078712000815 Published online by Cambridge University Press

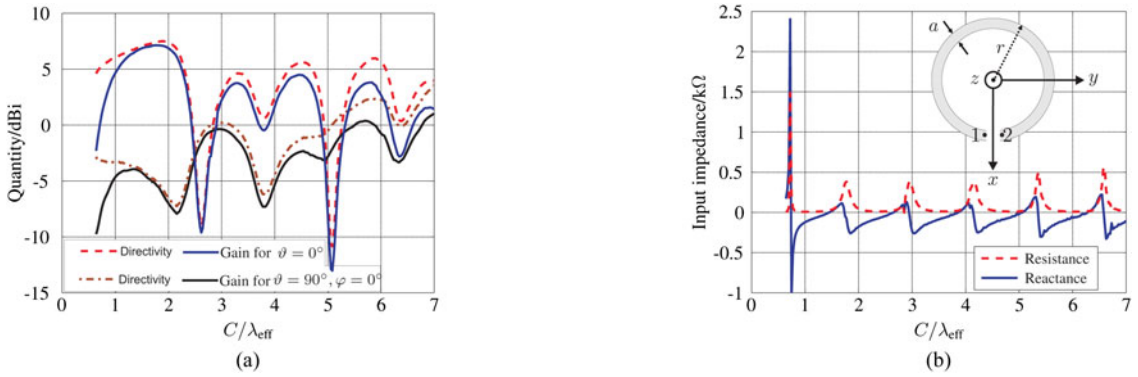

Fig. 13. Planar loop antenna in an 8 × 8 mm² eWLB package by 3D simulation at 76.5 GHz. (a) Directivity and gain versus loop perimeter and (b) Input impedance versus loop perimeter.

investigated the characteristics of the loop by changing its perimeter in an 8 × 8 mm² eWLB package and observing the gain in both the broadside, i.e., $\vartheta = 0^\circ$ and the end-fire direction at $\vartheta = 90^\circ$. The planar circular loop has a fixed strip width of $a = 187$ μm and a variable radius r as shown in Fig. 13(b). The feeding source is applied directly between points 1 and 2. Figure 13(a) shows the simulated gain and directivity, in both end-fire and broadside directions, versus the perimeter of loop normalized to the effective wavelength C/λ_{eff} within the package environment. It shows that the maximum gain in the broadside direction is achieved with a loop perimeter of $1.8\lambda_{eff}$. The gain is independent of the strip width as long as it is considerably smaller than the operating wavelength; e.g., the ratio of the strip width to the loop perimeter at $1.8\lambda_{eff}$ is about 4%. Figure 13(b) plots the real and the imaginary parts of impedance between point 1 and point 2. It also shows that the first and the only antiresonance occurs at a loop perimeter of $0.7\lambda_{eff}$. Therefore, the appropriate practical point of operation is the second resonance, i.e., the first series resonance, where the input impedance has a reasonable value for matching and the maximum gain is achieved. The gain as well as the input impedance can be determined by approximating the non-uniform current distribution over the loop by a Fourier series as in a conventional wire loop antenna [12]. In [6], a single PLA antenna with an inner perimeter of 2.85 mm is developed and measured in an 8 × 8 mm² eWLB package as shown in Fig. 14. The reference plane of the measurement and the simulation is the package edge. The measurement along the H-plane shows strong ripples compared to simulation. It is due to the parasitic radiation from the waveguide port, the CPS transmission line, and the PCB-to-package transition that are not included in the simulation. In addition, in practical applications, these transitions will be excluded and hence their effects. The distance between the antenna and the Si-chip is optimized to minimize the effect of the chip on the antenna efficiency.

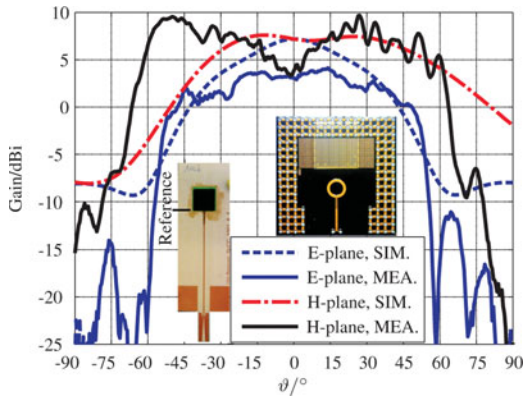

Fig. 14. Radiation pattern of PLA at 76 GHz [6].

B) Printed dipole antenna (PDA)

The inherent nature of a differential feed suggests the use of a dipole antenna as a good candidate for an AiP concept. A single PDA, supported by a reflector at a distance of 200 μm, was developed in an 8 × 8 mm² eWLB package. Figure 15(a). shows the measured and the simulated radiation pattern of a conventional PDA along the E-plane and the H-plane [6]. The measurements of different samples show a deformation in the H-plane pattern at positive ϑ-angles for the PDA. One way to better integrate a PDA in a package and to minimize the coupling in an antenna array configuration is to change the orientation of the dipole wings. Figure 15(b) shows the simulated and measured E-plane and H-plane radiation pattern of a PDA with 90-tilted wings. A lower gain is recorded in the broadside direction with a more pronounced dip in the H-plane. The dip is a result of the propagation through the mold compound. Increasing the mold thickness from 401 to 940 μm results in a dip level difference of 22 dB as shown in Fig. 5 for a PLA.

In a multichannel system, more than one antenna per package is needed. Therefore, we developed four PDAs in one package as shown in Fig. 16(a). This is a generic configuration that can be used in a wide range of applications such as a 4-channel radar system where the four channels are simultaneously powered on for transmission but receiving from each channel individually. In Fig. 16(a), the antennas are uniformly distant by 2.5 mm in an 8 × 12 mm² eWLB package. The geometrical structures of the antennas are identical. Also, a dummy Si-chip is centered along the width of the package. Figure 16(b) shows the simulation results of the reflection coefficient for each antenna and the coupling between them as well. It shows that all four antennas have almost the same resonance frequency. The drift in the resonance frequency is due to the different electrical length of each antenna, which stems from its position in the package and its interaction with the chip and the other antennas. The isolation between the different channels is always better than 18 dB. The isolation can be further improved by using a PLA or a

https://doi.org/10.1017/S1759078712000815 Published online by Cambridge University Press

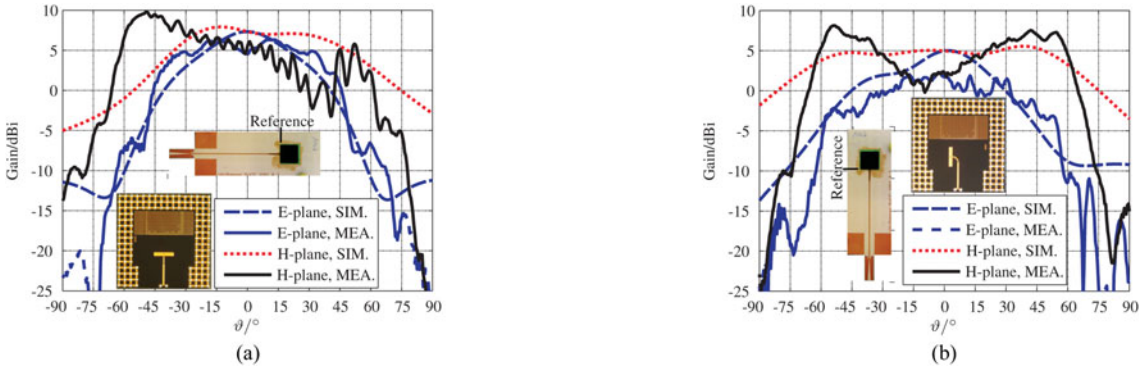

Fig. 15. Simulation and measurement results of PDA antennas in 8 × 8 mm² eWLB package. (a) PDA at 76 GHz [6] and (b) PDA with 90°-tillt 76 GHz.

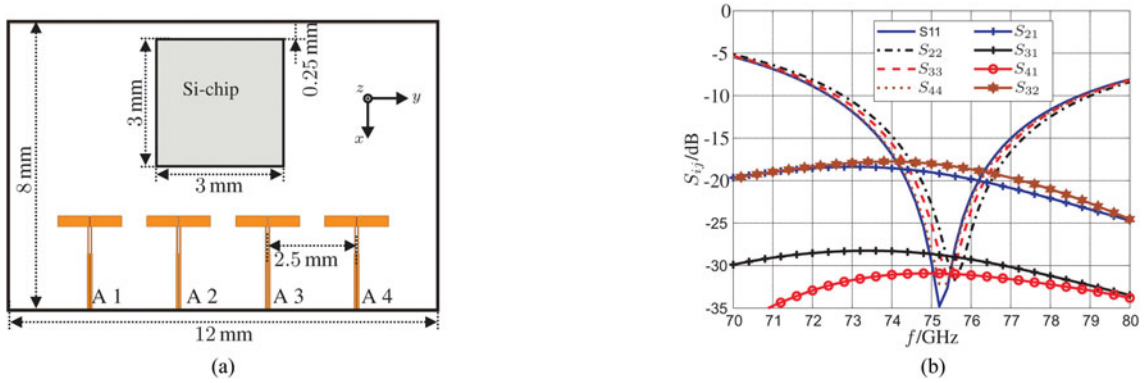

Fig. 16. Antenna array in 8 × 12 mm² eWLB package. (a) Four PDAs in an eWLB package and (b) Refelection coefficients and coupling.

tilted PDA. Figure 17 shows the radiation pattern when all elements are simultaneously fed with identical amplitudes and identical phases. The gain and the efficiency of the array antenna are 12.0 dBi and 79%, respectively. Figures 18(a) and 18(b) show the radiation pattern for each antenna while the other antennas are switched off, i.e., their ports are matched. It is observed that the H-planes of A 1 and A 4 are identical while their E-planes are mirrored due to their locations. Similarly, this behavior is observed for the inner two PDAs. Their H-planes are identical while their E-planes are mirrored along the *xz*-plane. The usage of the antenna array configuration and the addition of directors on top of the mold compound can improve the radiation characteristics.

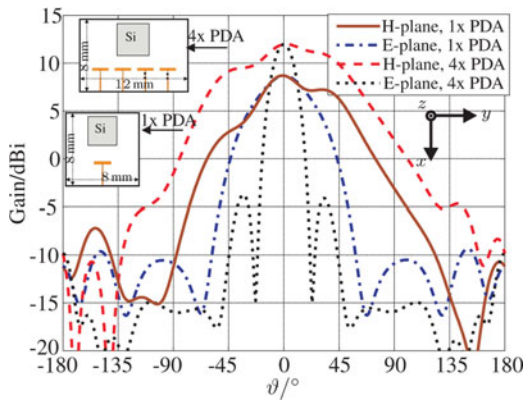

Fig. 17. Radiation pattern of four PDAs.

C) Gain enhancement

1) DIELECTRIC LENS

Using the antenna in package, an improved gain can be obtained with the aid of a dielectric lens that collimates the radiated waves. We used a dielectric lens with a diameter of 55 mm, mounted on top of the eWLB package at a distance $d = 25$ mm. Figure 19 shows the measured radiation pattern of a PDA antenna with and without the use of a dielectric lens. The usage of the lens increases the gain to 26.5 dBi and forms an HPBW of 4.5°. A tolerance in the distance d between the lens and the antenna by ± 1.5 mm leads to a gain diminution less than 0.5 dB. The choice of a proper lens enables the realization of different gains that suit the target application.

2) STACKED DIRECTIVE ELEMENTS

Increasing the effective aperture of an antenna increases its directivity and gain. This can be achieved by adding more elements in the plane of the antenna or in a vertical fashion. Similar to a Yagi-Uda antenna, directors are patterned on the top of the mold compound of an 8 × 8 mm² eWLB package as shown in Fig. 20(a) The distance between the fed PDA and the director, i.e., the mold thickness, is optimized together with the length and the width of the director to increase the gain of the antenna. The director has a length of $0.45\lambda_e$, where λ_e is the effective wavelength and a width of about $0.13\lambda_e$. Hence, the length of the director is 28% smaller than the directly fed PDA. The usage of the director increases the gain by 1.2 dB compared to a PDA in package

https://doi.org/10.1017/S1759078712000815 Published online by Cambridge University Press

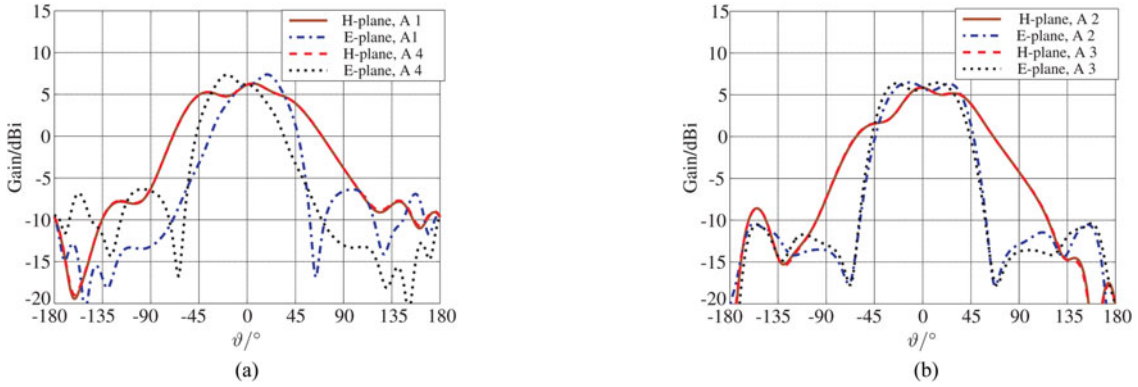

Fig. 18. Antenna array in an 8 × 12 mm² eWLB package. (a) Radiation pattern of PDA 1 and PDA 4 and (b) radiation pattern of PDA 2 and PDA 3.

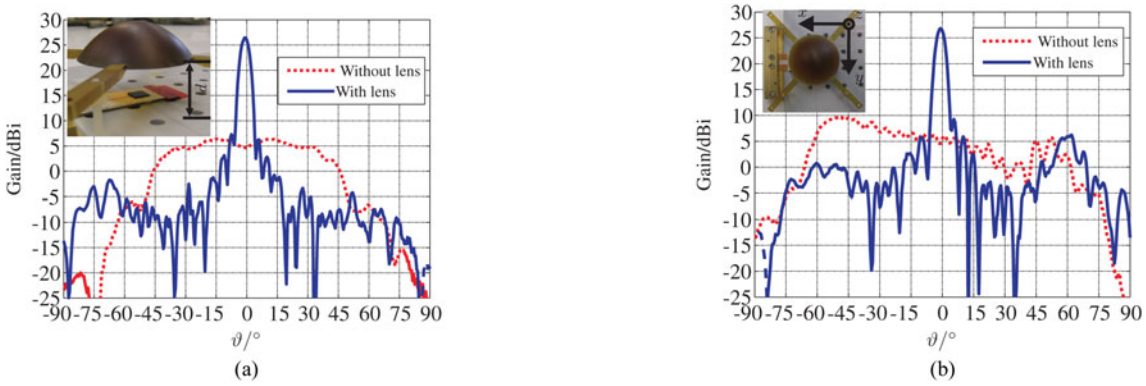

Fig. 19. PAD with a dielectric lens at a distance $d = 25$ mm. (a) E-plane (yz-plane) at 76 GHz and (b) H-plane (xz-plane) at 76 GHz.

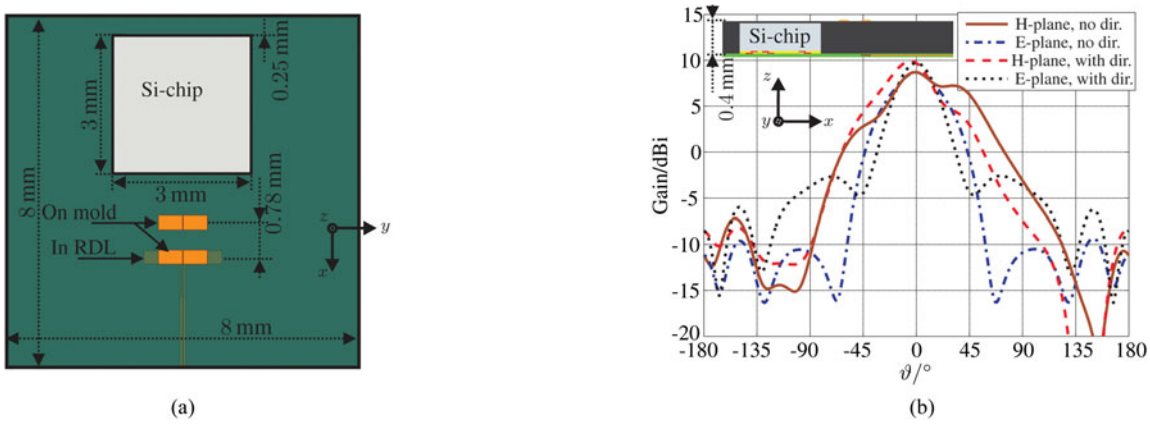

Fig. 20. An 8×8 mm² eWLB package with parasitic directors. (a) Top view of an eWLB package and (b) radiation pattern.

without directors as shown in Fig. 20(b). Furthermore, to enhance the radiation characteristics in the H-plane of the antenna, a second parasitic element is added along that plane. The antenna has a simulated gain and efficiency of about 9.9 dBi and 71%, respectively.

V. CONCLUSION

The study of the eWLB package as an antenna platform is carried out using two different package sizes 8 × 8 mm² and 8 × 12 mm². The sensitivity of the antenna characteristics to different aspects such as the package fabrication tolerance and its soldering process are addressed and discussed. Mainly, a variation of the soldering balls' height by ±30 μm has an impact of shifting the resonance frequency by about 3 GHz. Since the location of the Si-chip has also a strong impact on the antenna performance, its location has been optimized to minimize this effect. An acceptable performance has been observed while studying the effects of the Si-chip on the radiation characteristics of an AiP over the frequency range of 76–81 GHz. Design procedures for electrically large loops in package are introduced to enable a systematic design for such antennas. Furthermore, a PDA

https://doi.org/10.1017/S1759078712000815 Published online by Cambridge University Press

with 90°-tilted wings is developed and characterized. It can be used to minimize the coupling in an antenna array configuration. Also, the design and the characterization of four PDAs in one package are introduced. In addition, different techniques for gain enhancement of the AiP such as stacked elements, antenna array, and the usage of a dielectric lens are discussed. Using the array concept, the gain of a single element is increased by about 3 dB in a planar array and by 1.2 dB with a stacked director. The usage of a 55 mm dielectric lens with a single PDA in an $8 \times 8\ mm^2$ eWLB package records a measured gain of 26.5 dBi. A measurement concept for passive AiPs characterization is introduced, where a 77 GHz RF-transition, from the package to the PCB, is developed with an insertion loss of less than 1 dB. The antenna-in-eWLB packaging concept tends to have a wide impedance bandwidth of about 8 GHz and a measured gain in the range of 9 dBi per element. Overall, the eWLB package is viable as an antenna platform and is a strong candidate for a SiP concept. Further study of the package environment and the antenna radiation mechanism as well as the effect of different propagating modes in the plastic package are considered in future work.

ACKNOWLEDGEMENTS

We thank Infineon Technologies for the fabrication of the eWLB packages. We also acknowledge the financial support by the German Federal Ministry of Education and Research (BMBF) within the RoCC project.

REFERENCES

[1] Zhang, Y.P.; Duixian Liu. etc: Antenna-on-chip and antenna-in-package solutions to highly integrated millimeter-wave devices for wireless communications. IEEE Trans. Antennas Propag., **57** (10): (2009), 2830–2841.

[2] Hasch, J.; Wostradowski, U.; Gaier, S.; Hansen, T. etc: 77 GHz radar transceiver with dual integrated antenna elements. in German Microwave Conf., Berlin, Germany, March 2010, 280–283.

[3] Takeuchi, J.; Hirata, A.; Takahashi, H.; Kukutsu, N.: 10-Gbit/s bi-directional and 20-Gbit/s uni-directional data transmission over a 120-GHz-band wireless link using a finline ortho-mode transducer, in Microwave Conf. Proc. (APMC), 2010 Asia-Pacific, Yokohama, Japan, December 2010, 195–198.

[4] Lopez, A.V.; Papapolymerou, J.; Akiba, A.; Ikeda, K.; Mitarai, S.; Ponchak, G.: 60 GHz micromachined patch antenna for wireless applications, in IEEE Int. Symp. on Antennas and Propagation (APSURSI), Washington, USA, July 2011, 515–518, doi: 10.1109/APS.2011.5996758.

[5] Carrillo-Ramirez, R.; Jackson, R.W.: A Highly Integrated Millimeter-wave Active Antenna Array Using BCB and Silicon Substrate. IEEE Trans. Microw. Theory Tech., **52** (6) (2004), 1648–1653.

[6] Alhenawy, M.; Schneider, M.: Integrated antennas in eWLB packages for 77 GHz and 79 GHz automotive radar sensors, in 41st European Microwave Conf. (EuMC), Manchester, United kingdom, October 2011, 1312 –1315.

[7] Fischer, A.; Tong Ziqiang.; Hamidipour, A.; Maurer, L.; Stelzer, A.: A 77-GHz antenna in package, in 41st European Microwave Conf. (EuMC), Manchester, United kingdom, October 2011, 1316–1319.

[8] Brunnbauer, M.; Furgut, E.; Beer, G.; Meyer, T.: Embedded wafer level ball grid array (eWLB), in Eighth Electronics Packaging Technology Conf., EPTC '06, Singapore, December 2006, 1–5, doi: 10.1109/EPTC.2006.342681.

[9] Meyer, T.; Ofner, G.; Bradl, S.; Brunnbauer, M.; Hagen, R.: Embedded wafer level ball grid array (eWLB), in 10th Electronics Packaging Technology Conf., 2008. EPTC, Singapore, December 2008, 994–998, doi: 10.1109/EPTC.2008.4763559.

[10] Pressel, K.; et al.: Embedded wafer level ball grid array (eWLB) technology for system integration, in IEEE CPMT Symp. Japan, 2010, August 2010, 1–4, doi: 10.1109/CPMTSYMPJ.2010.5679657.

[11] Alhenawy, M.; Schneider, M.: Rectangular waveguide to coplanar stripline transition based on a unilateral finline, in Proc. Fourth European Conf. on Antennas and Propagation (EuCAP), Prague, Czech Republic, April 2012.

[12] Pocklington, H.C.: Electrical oscillations in wires, in Cambridge Philosophical Society Proc., University Press, volume 9, 1897, 324.

Mahmoud Alhenawy received his B.Sc. degree in Electronics and Communication Engineering from Mansoura University, Egypt, in 2005. In 2009, he earned his M.Sc. degree in Communication and Information Technology from the University of Bremen, Germany. Since May 2009, he has been working toward the PhD degree as a Research Assistant in the Institute of Telecommunications and High Frequency Techniques, RF & Microwave Engineering Laboratory, University of Bremen, Germany. His research interests include antenna systems and packaging techniques for automotive radar sensors in mm-wave band. Also, Mr Alhenawy conducts a research on realizing efficient antenna systems for 60 GHz communication links.

Martin Schneider received his Diploma and Doctorate degree in Electrical Engineering and Information Technology from the University of Hannover, Germany, in 1992 and 1997, respectively. From 1997 to 1999, he was with Bosch Telecom GmbH in Backnang, Germany, where he developed microwave components for point-to-point and point-to-multipoint radio link systems. In November 1999, he joined the Corporate Research and Advanced Development division of Robert Bosch GmbH in Hildesheim, Germany. As a project and section manager of the "Wireless Systems" group he focused on research and development of phased array and smart antenna concepts for automotive radar sensors at 24 and 77 GHz. From 2005 to 2006, Mr Schneider was with the business unit "Automotive Electronics of Robert Bosch GmbH in Leonberg, Germany. As a section manager he was responsible for the "RF electronics" for automotive radar sensors. Since March 2006, he has been a full professor and head of the RF & Microwave Engineering Laboratory at the University of Bremen, Germany. His research topics include RF front end circuits, millimeter wave circuits, and antenna systems at microwave and millimeter wave frequencies up to 170 GHz.